Area and thickness dependence of Auger recombination in nanoplatelets

John P. Philbin,[1] Alexandra Brumberg,[2] Benjamin T. Diroll,[3] Wooje Cho,[4] Dmitri V. Talapin,[3,4] Richard D. Schaller,[2,3] and Eran Rabani[1,5,6,a)]

[1)] *Department of Chemistry, University of California, Berkeley, California 94720, United States*

[2)] *Department of Chemistry, Northwestern University, Evanston, Illinois 60208, United States*

[3)] *Center for Nanoscale Materials, Argonne National Laboratory, Lemont, Illinois, 60439, United States*

[4)] *Department of Chemistry and James Franck Institute, University of Chicago, Illinois, 60637, United States*

[5)] *Materials Sciences Division, Lawrence Berkeley National Laboratory, Berkeley, California 94720, United States*

[6)] *The Sackler Center for Computational Molecular and Materials Science, Tel Aviv University, Tel Aviv, Israel 69978*

The ability to control both the thickness and the lateral dimensions of colloidal nanoplatelets offers a test–bed for area and thickness dependent properties in 2D materials. An important example is that of Auger recombination, which is typically the dominant process by which multiexcitons decay in nanoplatelets. Herein, we uncover fundamental properties of biexciton decay in nanoplatelets by comparing the Auger recombination lifetimes based on interacting and noninteracting formalisms with measurements based on transient absorption spectroscopy. Specifically, we report that electron–hole correlations in the initial biexcitonic state must be included in order to obtain Auger recombination lifetimes in agreement with experimental measurements and that Auger recombination lifetimes depend nearly linearly on the lateral area and somewhat more strongly on the thickness of the nanoplatelet. We also connect these scalings to those of the area and thickness dependencies of single exciton radiative recombination lifetimes, exciton coherence areas, and exciton Bohr radii in these quasi–2D materials.

Keywords: auger recombination, biexcitons, excitons, nanoplatelets

I. INTRODUCTION

Colloidal semiconductor nanoplatelets (NPLs) are quasi–2D materials with thicknesses that can be controlled with monolayer (ML) precision and lengths and widths that can be controlled on the nanometer scale.[1–3] The ability to vary the synthesis to separately yield NPLs of 2 through 8 ML thickness, with 3, 4, and 5 ML thicknesses the most well studied, opens the door to tuning the properties of the quasi–2D semiconductor NPL by just changing their thickness.[4–6] The most obvious property that can be tuned is that of the optical gap (i.e. absorption and emission energies), as the thickness is the primary determinant of the degree of quantum confinement in NPLs.[2,3,7,8] A more subtle aspect of the emission that also changes upon a change in the thickness is the rate of radiative recombination. Not only does the radiative recombination rate depend on the thickness, it also depends on the lateral area of the NPL.[9–11] An additional aspect related to applications of NPLs, ranging from lasers to photocatalysts, is that multiple excitons are required to be present in the NPL at the same time.[7,12–16] Thus, it is of general interest to understand how the lifetime of multiexcitonic states depends on the lateral area and thickness of NPLs.

Herein, we focus on the decay of biexcitonic states via Auger recombination (similar to exciton–exciton annihilation). Auger recombination (AR) is a nonradiative process in which one electron–hole pair recombines by transferring its energy to an additional quasiparticle (Fig. 1A) and is typically the dominant mechanism by which multiexcitonic states decay in semiconductor nanomaterials, making it of central importance to many nanomaterial–based applications.[17,18] Therefore, a fundamental understanding on how the AR lifetime (τ_{AR}) depends on the size and dimensionality of nanomaterials is of broad interest.

In quasi–0D quantum dots, the AR lifetime (see Eq. (1)) depends linearly on the nanocrystal volume and has become known as the "universal volume scaling law."[17,19–22] For quasi–1D nanomaterials, the AR lifetime scales linearly with the length of the nanorod and nearly quadratically with its diameter, thereby approximately following the universal volume scaling law.[22,23] The situation is somewhat more evolved for quasi–2D CdSe NPLs. Most recently, Li and Lian[24] reported that the AR lifetime scales linearly with the lateral area, $A = L_x L_y$ (see sketch in Fig. 1B). This linear dependence was rationalized by thinking of AR in NPLs as a classical collision of two particles in which the frequency of collision is limited by their spatial diffusion. Because electron–hole pairs are known to form bound Wannier excitons that are nearly spherical with average in–plane separation distances of approximately $1-2$ nm in CdSe NPLs,[25,26] the classi-

[a)] Electronic mail: eran.rabani@berkeley.edu

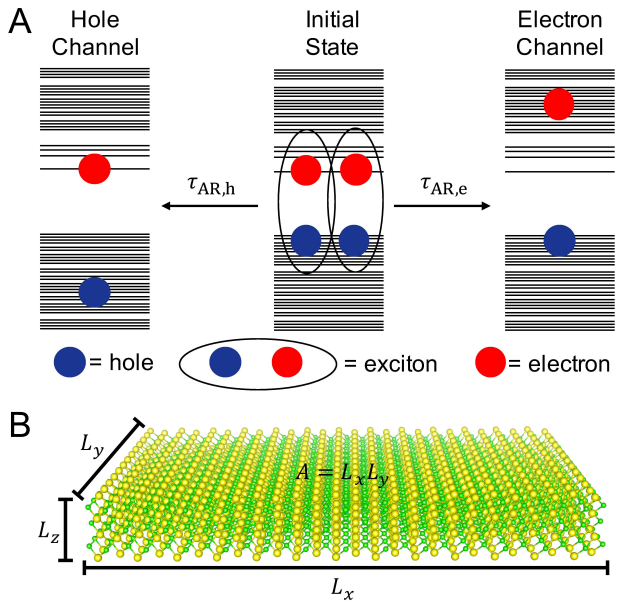

Figure 1. (A) Schematic of an Auger recombination event. The initial biexcitonic state is shown as two spatially uncorrelated excitonic states and the final states are shown as unbound electron–hole pairs. The hole (electron) channel on the left (right) shows the hole (electron) receiving a majority of the energy from the recombining exciton. (B) Representation of a 3 ML ($L_z = 0.91$ nm) CdSe nanoplatelet with $L_x = L_y = 8$ nm. Cd (Se) atoms are shown in yellow (green).

cal picture of AR as a collision between two independent particles where the particles are excitons is reasonable at first glance. Underlying this picture of AR are the assumptions that the biexciton binding energy is negligible such that the two excitons do not form a bound biexciton. And that the excitons are not coherent throughout the NPL and, therefore, diffuse in the NPL. A linear dependence of the AR lifetime on the lateral area was also recently reported for $CsPbBr_3$ perovskite NPLs.[27] These studies contradict an earlier report by She *et al.*[7] which found that the AR lifetimes are independent of area. It is important to note that the two studies on CdSe performed their studies using similarly sized NPLs.[7,24] In contrast to the volume (i.e. $\tau_{AR} \propto A^1$) or sub–volume ($\tau_{AR} \propto A^0$) scaling of AR lifetimes with respect to the lateral area of NPLs, the scaling of the AR lifetime as a function of the NPL thickness (L_z) or number of monolayers (MLs) was reported to obey a seventh power dependence, $\tau_{AR} \propto L_z^7$, in CdSe NPLs, a super–volume dependence.[24]

In this study, we provide an alternative mechanism that leads to similar area scaling for AR lifetimes in NPLs, which is based on the traditional scattering picture within lowest order perturbation theory coupling the initial biexcitonic state with the final electron–hole pair. A similar approach has been successfully applied to describe AR lifetimes in 0D quantum dots and quasi–1D nanorods, with very good agreement in comparison to experimental results over a wide range of system sizes.[22] Here, we focus on the regime $A \leq 100\ \text{nm}^2$ which is suitable for this coherent scattering picture and study the AR lifetimes for different CdSe NPLs shapes and thicknesses by applying our recently developed stochastic approach.[28] We uncover the underlying physics that cause the particular scaling in this coherent scattering picture. In addition, we analyze the thickness–dependent AR lifetimes in quasi–2D NPLs (as well as other properties, such as electron and hole kinetic energy, exciton binding energy, exciton Bohr radius, and screening), and provide reasonings for the mild thickness dependence observed in the coherent scattering picture as well as in other experiments on similar NPLs.

II. COMPUTATIONAL METHOD

AR is commonly described as a Coulomb–mediated scattering process for which an initial biexcitonic state ($|B\rangle$) of energy E_B decays into a final excitonic state ($|S\rangle$) of energy E_S via Coulomb (V) scattering (Fig. 1). An AR lifetime (τ_{AR}) for a nanostructure can be calculated using Fermi's golden rule where we average over thermally distributed initial biexcitonic states and sum over all final decay channels into single excitonic states:[22,29]

$$\tau_{\text{AR}}^{-1} = \sum_B \frac{e^{-\beta E_B}}{Z_B} \left[\frac{2\pi}{\hbar} \sum_S \left| \langle B | V | S \rangle \right|^2 \delta\left(E_B - E_S\right) \right] \quad (1)$$

In the above, the delta function ($\delta\left(E_B - E_S\right)$) enforces energy conservation between the initial and final states and the partition function (Z_B) is for the initial biexcitonic states (we assume biexcitons follow Boltzmann statistics). Utilizing the interacting, exciton–based framework, previously developed by Philbin and Rabani,[22] a deterministic calculation of an AR lifetime can be performed using

$$\tau_{\text{AR}}^{-1} = \tau_{\text{AR,e}}^{-1} + \tau_{\text{AR,h}}^{-1} \quad (2)$$

$$\tau_{\text{AR,e}}^{-1} = \frac{2\pi}{\hbar Z_B} \sum_B e^{-\beta E_B} \sum_{a,i} \left| \sum_{b,c,k} c_{b,i}^B c_{c,k}^B V_{abck} \right|^2 \delta\left(E_B - E_S\right)$$

$$\tau_{\text{AR,h}}^{-1} = \frac{2\pi}{\hbar Z_B} \sum_B e^{-\beta E_B} \sum_{a,i} \left| \sum_{j,c,k} c_{a,j}^B c_{c,k}^B V_{ijck} \right|^2 \delta\left(E_B - E_S\right),$$

where $E_S = \varepsilon_a - \varepsilon_i$ and V_{rsut} is the Coulomb coupling given by

$$V_{rsut} = \iint \frac{\phi_r\left(\mathbf{r}\right) \phi_s\left(\mathbf{r}\right) \phi_u\left(\mathbf{r}'\right) \phi_t\left(\mathbf{r}'\right)}{|\mathbf{r} - \mathbf{r}'|} d^3\mathbf{r}\, d^3\mathbf{r}'. \quad (3)$$

In the above equations, $\phi_r\left(\mathbf{r}\right)$ are quasiparticle states for electrons ($r \in a, b, c, ...$) or holes ($r \in i, j, k, ...$) and the coefficients ($c_{c,k}^B$) in Eq. (2) are determined by solving the Bethe–Salpeter equation.[30] The above approach includes spatial correlations within the electron–hole pairs

but ignores correlations between the excitons[31] and in the final electron–hole pair. It was previously shown that this interacting formalism predicts quantitively accurate AR lifetimes for quantum dots, nanorods and core/shell quantum dots.[22,28] On the other hand, noninteracting formalisms that ignore all electron–hole interactions in the initial biexcitonic state do not predict accurate AR lifetimes except for quantum dots in the very strong confinement regime[29] — highlighting the importance of exciton formation in nanocrystals. However, a major drawback of the interacting formalism for calculating AR lifetimes (Eq. (2)) is the computational cost, which scales with the system size (N) as $O\left(N^5\right)$. To reduce the computational cost, we utilize a stochastic formulation of Eq. (2) to calculate AR lifetimes for the CdSe NPLs studied in this work:[28]

$$\begin{aligned}
\tau_{\mathrm{AR}}^{-1} &= \tau_{\mathrm{AR,e}}^{-1} + \tau_{\mathrm{AR,h}}^{-1} \\
\tau_{\mathrm{AR,e}}^{-1} &= \frac{2\pi}{\hbar Z_B} \sum_B e^{-\beta E_B} \left\langle \left\langle \sum_b c^B_{b,i^A} R^{\zeta'}_{\theta^A b} \sum_{c,k} c^B_{c,k} R^{\zeta'}_{ck} \right\rangle^*_{\zeta'} \left\langle \sum_b c^B_{b,i^A} R^{\zeta}_{\theta^A b} \sum_{c,k} c^B_{c,k} R^{\zeta}_{ck} \right\rangle_{\zeta} \right\rangle_A \\
\tau_{\mathrm{AR,h}}^{-1} &= \frac{2\pi}{\hbar Z_B} \sum_B e^{-\beta E_B} \left\langle \left\langle \sum_j c^B_{a^I,j} R^{\zeta'}_{\theta^I j} \sum_{c,k} c^B_{c,k} R^{\zeta'}_{ck} \right\rangle^*_{\zeta'} \left\langle \sum_j c^B_{a^I,j} R^{\zeta}_{\theta^I j} \sum_{c,k} c^B_{c,k} R^{\zeta}_{ck} \right\rangle_{\zeta} \right\rangle_I .
\end{aligned} \tag{4}$$

In Eq. (4), the indices θ^A, i^A and a^I, θ^I are sampled final states from the complete set of single excitonic states (a, i pairs) in Eq. (2) and the notation $\langle ... \rangle_\zeta$ denotes an average over N_s stochastic orbitals. The R^ζ_{rs} matrices are calculated using

$$R^\zeta_{rs} = \int \phi^*_r(\mathbf{r})\, \phi^*_s(\mathbf{r})\, \theta^\zeta(\mathbf{r})\, d^3\mathbf{r}, \tag{5}$$

where $\theta^\zeta(\mathbf{r})$ is a stochastic representation of the Coulomb integral given by[32]

$$\theta^\zeta(\mathbf{r}) = \frac{1}{(2\pi)^3} \int d\mathbf{k}\, \sqrt{\widetilde{u}_\mathrm{C}(\mathbf{k})}\, \mathrm{e}^{\mathrm{i}\varphi(\mathbf{k})}\, \mathrm{e}^{\mathrm{i}\mathbf{k}\cdot\mathbf{r}} \tag{6}$$

where $\varphi(\mathbf{k})$ is a random phase between 0 and 2π at each k–space grid point, $\widetilde{u}_\mathrm{C}(\mathbf{k}) = 4\pi/k^2$ is the Fourier transform of the Coulomb potential. The computational cost of Eq. (4) is drastically lower than Eq. (2) for large systems sizes, scaling as $O\left(N^2\right)$ instead of $O\left(N^5\right)$. For more details on the computational methods, see our previous works.[22,28]

III. RESULTS

A. Comparison to experimental measurements

To begin to understand biexciton AR in CdSe NPLs, we compare the calculated AR lifetimes using both a noninteracting, free carrier–based formalism and an interacting, exciton–based formalism[28] to experimental measurements performed herein using transient absorption spectroscopy and to past measurements[7,24] for 4 ML (L_z = 1.21 nm) CdSe NPLs with various lateral areas ($A = L_x L_y$). NPLs were synthesized according to previous reports[7,33,34] using reaction time and temperature to adjust the lateral areas, later determined via transmission electron microscopy. For transient absorption measurements, samples were excited at 1 kHz using the 400 nm, frequency–doubled output of a 35 fs Ti:sapphire laser and probed using white light generated by passing 800 nm light through a sapphire plate. Scans were acquired at fluences corresponding to very low ($\langle N_\mathrm{exc}(t=0)\rangle \ll 0.1$) to moderate ($\langle N_\mathrm{exc}(t=0)\rangle \approx 0.2-0.5$) average number of initial excitons ($\langle N_\mathrm{exc}(t=0)\rangle$). Kinetics at the bleach maximum were normalized at $1.5-2.0$ ns, where dynamics are dominated by single exciton recombination, and then differenced to separate out biexciton–only dynamics. Biexciton dynamics were fit to a single exponential, and this process was repeated for multiple measurements at moderate fluences to yield an average AR lifetime.

As expected, the inclusion of electron–hole correlations in the initial biexcitonic state drastically impacts both the predicted AR lifetimes and scaling of the AR lifetimes with respect to the NPL lateral area. Specifically, Fig. 2 shows that the noninteracting (free carrier–based) method predicts AR lifetimes that are $1-2$ orders of magnitude longer than those predicted by the interacting, exciton–based formalism (Eq. (2)). For example, the AR lifetime of the 4 ML ($L_z = 1.2$ nm) CdSe NPL with $L_x = 4$ nm and $L_y = 10$ nm has a calculated AR lifetime of ~ 3800 ps using the free carrier–based formalism and an AR lifetime of ~ 90 ps using the exciton–based formalism. Fig. 2 also highlights the general accuracy of the atomistic electronic structure calculations. Specifically, exciton–based AR lifetime (green circles) calculations appear to provide quantitative agreement compared to our measurements (black squares) and previous measurements (blue and brown squares).[7,24] Importantly, both theory and experiments predict an increase in the AR lifetime as the area of the NPL increases for

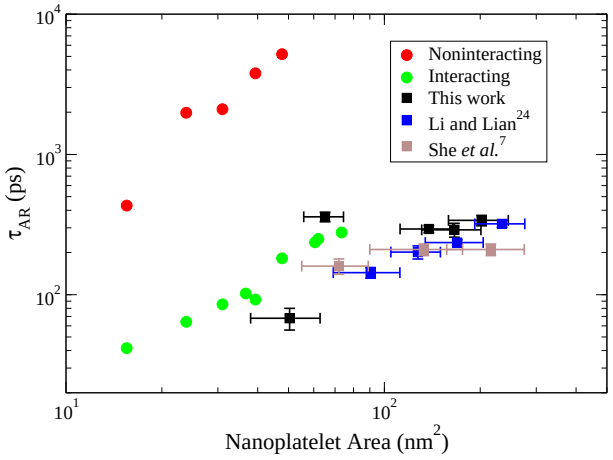

Figure 2. Biexciton Auger recombination lifetimes (τ_{AR}) for 4 ML CdSe NPLs calculated using both noninteracting, free carrier–based (red circles) and interacting, exciton–based (green circles) formalisms. The AR lifetimes predicted by the free carrier–based formalism are $1-2$ orders of magnitude longer than those predicted by the exciton–based formalism and those measured experimentally.[7,24] The experimentally measured lifetimes are shown using square symbols and calculated lifetimes are shown using circular symbols.

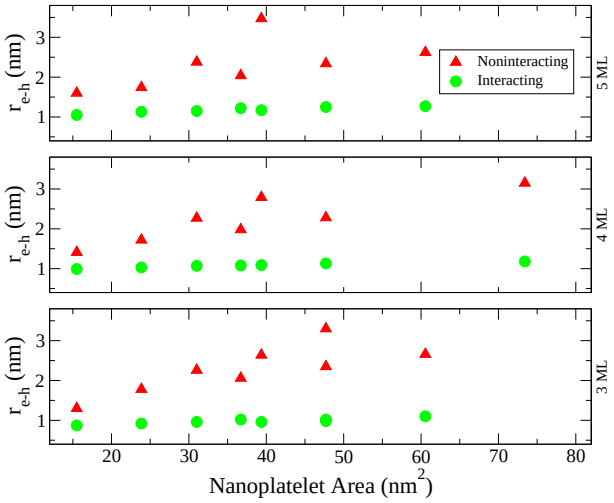

Figure 3. Root–mean–square exciton radii ($r_{\text{e-h}} = \sqrt{\langle(\mathbf{r}_{\mathrm{e}}-\mathbf{r}_{\mathrm{h}})^2\rangle}$) for 3 ML (bottom), 4 ML (middle), and 5 ML (top) thick CdSe NPLs as a function of the area of the NPLs. The red triangles show the calculated value using noninteracting (i.e. free–carrier) electron–hole pair states and the green circles show the calculated value using the interacting (i.e. excitonic) electron–hole pair states.

$A \leq 100$ nm^2. For larger lateral areas, at this point not accessible by the current theory, there seems to be a change in behavior in some of the experiments (see discussion below).

The disagreement between the free carrier–based and exciton–based formalisms arises from two primary reasons. The first is that the attractive Coulomb interaction that is responsible for exciton formation between the band–edge electron and band–edge hole mixes in band–edge states that have large momentums into the lowest energy excitonic states which facilitates momentum conservation in Auger processes.[24,35] The second reason derives from the free carrier–based formalism neglecting the large electron–hole attractive interaction on the single exciton level. This leads to an overestimation of the exciton Bohr radius ($a_{\mathrm{B,exc}}$) and the root–mean–square exciton radius ($r_{\text{e-h}} = \sqrt{\left\langle(\mathbf{r}_{\mathrm{e}}-\mathbf{r}_{\mathrm{h}})^2\right\rangle}$ where $\mathbf{r}_{\mathrm{e}}$ and $\mathbf{r}_{\mathrm{h}}$ are the coordinates of the electron and hole, respectively) when electron–hole interactions are ignored. Fig. 3 shows that the noninteracting formalism predicts that $r_{\text{e-h}}$ is nearly proportional to the square root of the NPL area, and, in contrast, that $r_{\text{e-h}}$ is nearly independent of the NPL area when electron–hole interactions are taken into account by solving the Bethe-Salpeter equation as is done using the interacting formalism. This overestimation of $r_{\text{e-h}}$ by noninteracting formalisms leads to an underestimation of the Coulomb matrix elements in Eq. (3) and, thus, an overestimation of AR lifetimes by free carrier–based formalisms (Fig. 2).

B. Lateral area dependence of Auger recombination

Fig. 4 shows a nearly linear dependence of the AR lifetimes on the lateral area ($A = L_x L_y$) for 3, 4, and 5 ML CdSe NPLs. The linear dependence on the NPL area is in agreement with recent experimental reports for both CdSe NPLs and $CsPbBr_3$ perovskite NPLs.[24,27] Interestingly, both the coherent scattering mechanism used in our calculations and the exciton diffusion–based model[24] described previously lead to linear dependencies with the lateral area.

The results of She *et al.*[7] are not necessarily at odds with this linear dependence. In fact, She *et al.* reported that the AR lifetime increases upon increasing the lateral area of 4 ML CdSe NPLs from 72 nm^2 to 133 nm^2, which is consistent with results presented in this work for the size regime that we focus on ($A \leq 100$ nm^2). At larger areas, She *et al.* reported a plateau of the AR lifetime, whereas Li and Lian[24] do not observe a plateauing of the AR lifetime, even for NPLs with lateral areas greater than 200 nm^2. At this point, our computational technology is still limited to the size regime of $A \leq 100$ nm^2 and further developments are required to address larger areas.

C. Thickness dependence of Auger recombination

An important aim of this work was to determine and understand the prediction of the exciton–based, interacting formalism for the thickness (L_z) dependence of AR in CdSe NPLs. The only previous experimental work on

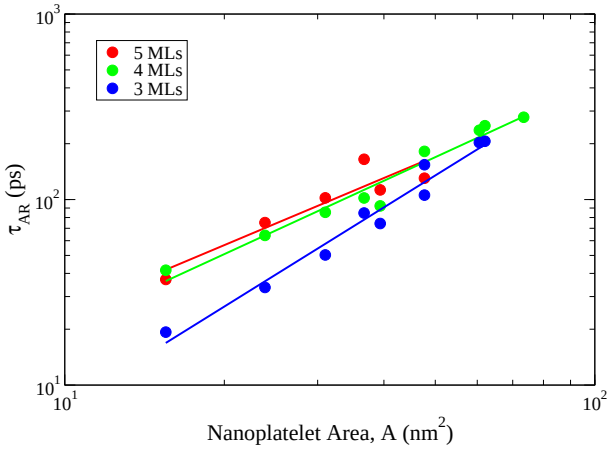

Figure 4. Auger recombination lifetimes, τ_{AR}, for CdSe NPLs as a function of the area of the NPL. Power law fits, $\tau_{AR} \propto A^{\alpha}$, are also shown for each set of AR lifetimes with $\alpha = 1.2, 1.3$, and 1.8 in descending ML thickness.

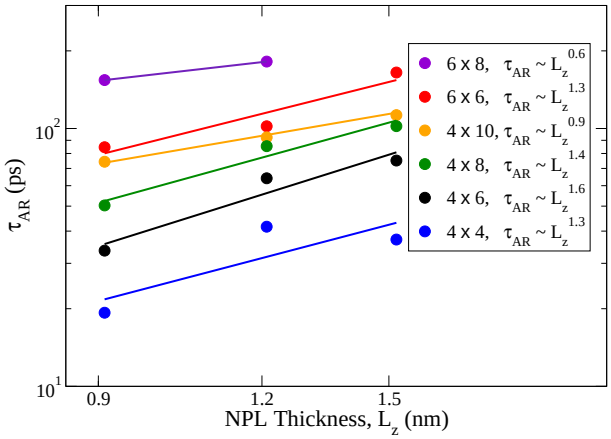

Figure 5. Auger recombination lifetimes (τ_{AR}) for CdSe NPLs as a function of the thickness of the NPL. Power law fits, $\tau_{AR} \propto L_z^{\gamma}$, are also shown for each set of AR lifetimes. The lateral dimensions are shown as $L_x \times L_y$ in nm.

this found a seventh power dependence ($\tau_{AR} \propto L_z^7$). Fig. 5 shows the calculated AR lifetime as a function of the thickness for six different lateral dimensions that were kept fixed upon changing the thickness. The power law fits for each set of three thicknesses studied here (corresponding to 3, 4, and 5 MLs) give a calculated AR lifetime dependence on the thickness ranging from 0.6 to 1.6 ($\tau_{AR} \propto L_z^{0.6-1.6}$). While this is a rather large range of power dependence on thickness, it is certainly a milder dependence than reported previously.[24] In fact, it is rather close to the scaling that would be predicted by the universal volume scaling law (i.e. $\tau_{AR} \propto L_z^{1.0}$). The increase of the AR lifetime upon increasing NPL thickness is intuitive as thinner NPLs have larger exciton binding energies and smaller exciton Bohr radii. Both of these result in an increase of the Coulomb coupling matrix elements which overtakes the decrease in the density of states, thus leading to shorter AR lifetimes for thinner NPLs.

Experimentally, it is difficult to perform a systematic study of the thickness dependence, as control over NPL lateral area is more difficult to achieve than thickness control. In particular, 3 ML NPLs tend to have larger lateral dimensions than those of 4 and 5 ML CdSe NPLs using presently available syntheses, making it difficult to compare thickness independent of lateral area.[7,36,37] That being said, we determined AR lifetimes for many 4 and 5 ML CdSe NPLs and consistently found longer AR lifetimes for the 5 ML NPLs, which is also consistent with the work of She *et al.*[7] and Li and Lian.[24] Therefore, we conclude that AR lifetimes increase upon increasing thickness based on our experimental measurements and calculations; however, we believe that the dependence on the thickness is milder than previously reported.[24]

IV. DISCUSSION

A. Lateral area dependence

We begin the discussion of the lateral area dependence of AR lifetimes predicted by our Coulomb–mediated scattering approach by introducing an important concept of the exciton coherence area (A_{exc}) and its lateral area dependence in CdSe NPLs. The exciton coherence area is a measure of the area over which the center of mass of the exciton undergoes coherent motion.[38,39] An implicit assumption of our model (Eq. (2)) is that the two excitonic states that comprise the initial biexcitonic state are coherent throughout the NPL. This is shown pictorially in Fig. 6. Specifically, the electron (red) and hole (blue) densities without (top panel) and with (bottom panel) electron–hole interactions included in the calculation of the low lying excitonic states are shown for a 3 ML ($L_z = 0.91$ nm) CdSe NPL with $L_x = L_y = 8$ nm. It can be seen in Fig. 6 that in both the noninteracting and interacting cases the electron and hole densities look similar: they both are delocalized over almost the entire NPL area and the electron density is composed primarily of S–type atomic orbitals and the hole density is composed primarily of P–type atomic orbitals. The delocalization of their projected densities and similar spatial extent suggest that the exciton center–of–mass coherence area is similar and is almost equal to the entire size of the NPL. This result makes sense as our calculations were performed with the 0 K atomic configuration and, even if considered at room temperature, the exciton coherence area measured experimentally is greater than or equal to the NPL areas for which we have calculated AR lifetimes.[39,40]

The fact that the exciton is coherent throughout the entire NPL highlights the wave–like nature of electron–hole pairs in CdSe NPLs. As a side note, this wave–like

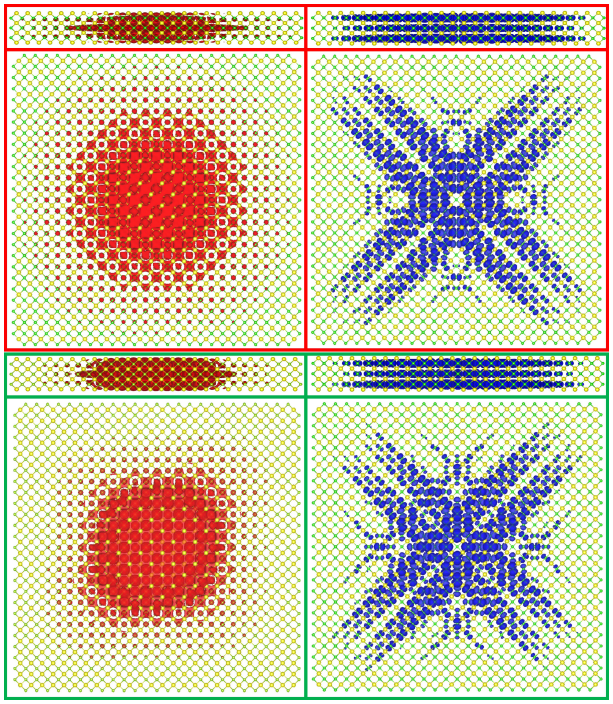

Figure 6. Electron (red) and hole (blue) carrier densities for the lowest lying noninteracting (top, red box) and interacting (bottom, green box) excitonic state for a 3 ML (L_z = 0.91 nm) CdSe nanoplatelet with $L_x = L_y$ = 8 nm. The quasiparticle densities are integrated over all possible locations of the other quasiparticle for the interacting (i.e. correlated electron–hole pair state). The densities are visualized by looking down the x–axis and z–axis to show that the exciton coherence areas extend throughout a majority of the NPLs and the total area does not change much upon inclusion of electron–hole correlations.

nature of electron–hole pairs is also very important in single exciton decay as it, together with the small average electron–hole separations shown in Fig. 3, is responsible for the giant oscillator strengths of NPLs as the radiative decay rate is proportional to the ratio of the exciton coherence area to the square of the exciton Bohr radius.[10,41–43] In terms of our calculations of AR lifetimes, the linear dependence of the AR lifetime on the lateral area observed in our calculations arises from the Coulomb coupling between initial biexcitonic states and final excitonic states decreasing upon increasing area and not from the collision frequency of the two excitons decreasing upon increasing area as previously used to explain the measured linear area dependence.[24,27] Thus, the measurement of a linear area dependence cannot distinguish between the two mechanisms, and the coherent mechanism developed here is an alternative picture that seems consistent with the exciton coherent areas of the CdSe NPLs studied in this work ($A \leq 100$ nm^2).[39,40]

Switching our focus to the disagreement with an earlier report that measured area–independent AR lifetimes,[7] the question that arises is why the exciton–based formalism given in Eq. (2) predicts a linear dependence and not an area independent AR lifetime? This can be addressed by analyzing the initial biexcitonic states. In Eq. (2), the initial biexcitonic state is given by

$$|B\rangle^{\text{exc}} = \sum_{b,j}\sum_{c,k} c_{b,j}c_{c,k}a_b^\dagger a_j a_c^\dagger a_k \left|0\right\rangle \otimes \left|\chi_B\right\rangle, \qquad (7)$$

where $|B\rangle^{\text{exc}}$ denotes the initial biexcitonic state within the exciton–based (interacting) formalism and $|\chi_B\rangle$ is the spin part of the biexciton. Eq. (7) does not include spatial correlations between the excitonic states; correlations are only included within the single excitons by the two index coefficients ($c_{b,j}$ and $c_{c,k}$). On the other hand, a fully–correlated biexcitonic state,

$$|B\rangle^{\text{biexc}} = \sum_{b,j,c,k} c_{b,j,c,k}a_b^\dagger a_j a_c^\dagger a_k \left|0\right\rangle \otimes \left|\chi_B\right\rangle, \qquad (8)$$

includes spatial correlations between all four quasiparticles by using four index coefficients, ($c_{b,j,c,k}$). Unfortunately, the calculation of the four index coefficients in Eq. (4) is currently not feasible for NPLs. However, the biexciton binding energy is believed to be comparable to $k_{\text{B}}T$ at room temperature where k_{B} is the Boltzmann constant and T is the temperature in CdSe nanocrystals[44] and quasi–2D materials,[7,45] implying that two excitons do not bind to form a stable biexciton. Thus, the combination of large coherence lengths of single excitons on the order of hundreds of nanometers in II–VI 2D materials[38] and the relatively small biexciton binding energies should make Eq. (7) a good approximation of the initial biexcitonic states involved in AR. If, on the other hand, the biexciton binding energy were large[7,12,46] and the lateral dimensions of the NPL were larger than the biexciton Bohr radius, then one could imagine that the initial biexcitonic state would stop changing as the NPL lateral dimensions increase beyond the biexciton Bohr radius. This could lead to a plateauing of the AR lifetime with increasing lateral area. Currently, it is unclear if this is the regime the experiments have been in ($A \sim 200$ nm^2 and T = 298 K).

B. Thickness dependence

An important aspect of the calculations shown in Fig. 5 is that the dielectric constant (ϵ) used to obtain the coefficients ($c^B_{c,k}$) in Eq. (4) by solving the Bethe–Salpeter equation was set to a fixed value of 5 for all NPLs. We believe that the use of $\epsilon = 5$ is justified because the screening in the Bethe–Salpeter equation arises from the electron motion (i.e., not the ions) and the larger optical gap of confined systems combine to reduce the screening compared to bulk CdSe. That being said, we calculated the AR lifetime for NPLs with $L_x = L_y = 6$ nm for the three thicknesses ($L_z = 0.91, 1.21, 1.52$ nm) for dielectric constants ranging from 4 to 6 to test if these changes in the dielectric constant would change the predicted thickness dependence of AR lifetimes in CdSe NPLs. If we

were to assume that the dielectric constants were 4 for 3 ML NPLs, 5 for 4 ML NPLs, and 6 for 5 ML NPLs, the thickness dependence is $\tau_{AR} \propto L_z^2$, suggesting that dielectric changes can make the thickness dependence of AR lifetimes a bit steeper in NPLs. However, this is a far from comprehensive study on how the dielectric constant changes as a function of NPL thickness and how these changes impact AR lifetimes. Furthermore, our calculations neglect the dielectric mismatch between the NPLs and the surrounding environment, which is known to have important consequences on the electronic structure of excitons in NPLs.[47–49] Altogether, this suggests a more detailed investigation of the impact of dielectric changes and dielectric mismatch on AR lifetimes in nanomaterials along with more experiments to better understand the scaling with respect to the NPL thickness.

V. CONCLUSIONS

In summary, we report the first atomistic, electronic structure based calculations of AR lifetimes in quasi–2D NPLs. We find that electron–hole correlations in the initial biexcitonic state are necessary to obtain AR lifetimes that are in agreement with experimental measurements. The AR lifetimes show an increase with the lateral area for NPLs in the regime $A \leq 100$ nm^2 according to both our theory and current and previous measurements.[7,24] For larger lateral areas ($A \geq 150$ nm^2), not accessible by current computational technology, two distinct behaviors were observed. The current work suggests that AR lifetimes plateau with increasing area, consistent with the measurements of She *et al.*,[7] while previous experiments observed a linear increase with area.[24,27] The linear increase of the AR lifetime with area was previously explained using an exciton diffusion–based mechanism.[24,27] Our theory provides an alternative explanation based on a coherent scattering mechanism that seems consistent with exciton coherent lengths in CdSe NPLs[40] and shows a nearly linear increase of AR lifetimes with lateral area. In addition, we find that the AR lifetimes depend on the NPL thickness with a power law of L_z^{1-2}, depending on the shape of the NPL, which is milder than previously reported.[24] This milder thickness dependence together with the nearly linear lateral area dependence are consistent with the universal volume scaling law observed in quasi–0D quantum dots and quasi–1D nanorods.[17,19,22,23]

ACKNOWLEDGMENTS

This work was supported by the National Science Foundation DMREF Program under awards DMR–1629361, DMR–1629601, and DMR–1629383 and by the Graduate Research Fellowship Program under Grant No. DGE–1324585 (A.B.). E.R. also acknowledges the University of California Lab Fee Research Program (Grant LFR–17–477237 and the National Energy Research Scientific Computing Center (NERSC), a U.S. Department of Energy Office of Science User Facility operated under Contract No. DE–AC02–05CH11231. Use of the Center for Nanoscale Materials, an Office of Science user facility, was supported by the U.S. Department of Energy, Office of Science, Office of Basic Energy Sciences, under contract No. DE–AC02–06CH11357.

REFERENCES

[1] S. Ithurria and B. Dubertret, J. Am. Chem. Soc. **130**, 16504 (2008).
[2] S. Ithurria, M. D. Tessier, B. Mahler, R. P. Lobo, B. Dubertret, and A. L. Efros, Nat. Mater. **10**, 936 (2011).
[3] M. D. Tessier, C. Javaux, I. Maksimovic, V. Loriette, and B. Dubertret, ACS Nano **6**, 6751 (2012).
[4] S. Ithurria, G. Bousquet, and B. Dubertret, J. Am. Chem. Soc. **133**, 3070 (2011).
[5] W. Cho, S. Kim, I. Coropceanu, V. Srivastava, B. T. Diroll, A. Hazarika, I. Fedin, G. Galli, R. D. Schaller, and D. V. Talapin, Chem. Mater. **30**, 6957 (2018).
[6] S. Christodoulou, J. I. Climente, J. Planelles, R. Brescia, M. Prato, B. Martín-Garciá, A. H. Khan, and I. Moreels, Nano Lett. **18**, 6248 (2018).
[7] C. She, I. Fedin, D. S. Dolzhnikov, P. D. Dahlberg, G. S. Engel, R. D. Schaller, and D. V. Talapin, ACS Nano **9**, 9475 (2015).
[8] Q. Zhou, Y. Cho, S. Yang, E. A. Weiss, T. C. Berkelbach, and P. Darancet, Nano Lett. **19**, 7124 (2019).
[9] M. Olutas, B. Guzelturk, Y. Kelestemur, A. Yeltik, S. Delikanli, and H. V. Demir, ACS Nano **9**, 5041 (2015).
[10] A. Naeem, F. Masia, S. Christodoulou, I. Moreels, P. Borri, and W. Langbein, Phys. Rev. B **91**, 121302 (2015).
[11] S. Bose, Z. Song, W. J. Fan, and D. H. Zhang, J. Appl. Phys. **119**, 143107 (2016).
[12] J. Q. Grim, S. Christodoulou, F. Di Stasio, R. Krahne, R. Cingolani, L. Manna, and I. Moreels, Nat. Nanotechnol. **9**, 891 (2014).
[13] C. She, I. Fedin, D. S. Dolzhnikov, A. Demortière, R. D. Schaller, M. Pelton, and D. V. Talapin, Nano Lett. **14**, 2772 (2014).
[14] Q. Li, Z. Xu, J. R. McBride, and T. Lian, ACS Nano **11**, 2545 (2017).
[15] M. Pelton, J. Phys. Chem. C **122**, 10659 (2018).
[16] B. Guzelturk, M. Pelton, M. Olutas, and H. V. Demir, Nano Lett. **19**, 277 (2019).
[17] V. I. Klimov, A. A. Mikhailovsky, D. W. McBranch, C. A. Leatherdale, and M. G. Bawendi, Science **287**, 1011 (2000).
[18] V. I. Klimov, Annual Review of Condensed Matter Physics **5**, 285 (2014).
[19] V. I. Klimov, J. A. McGuire, R. D. Schaller, and V. I. Rupasov, Phys. Rev. B **77**, 195324 (2008).
[20] I. Robel, R. Gresback, U. Kortshagen, R. D. Schaller, and V. I. Klimov, Phys. Rev. Lett. **102**, 177404 (2009).
[21] L. A. Padilha, J. T. Stewart, R. L. Sandberg, W. K. Bae, W.-k. Koh, J. M. Pietryga, and V. I. Klimov, Nano Lett. **13**, 1092 (2013).
[22] J. P. Philbin and E. Rabani, Nano Lett. **18**, 7889 (2018).
[23] H. Htoon, J. A. Hollingsworth, R. Dickerson, and V. I. Klimov, Phys. Rev. Lett. **91**, 227401 (2003).
[24] Q. Li and T. Lian, Nano Lett. **17**, 3152 (2017).
[25] R. Scott, A. W. Achtstein, A. V. Prudnikau, A. Antanovich, L. D. A. Siebbeles, M. Artemyev, and U. Woggon, Nano Lett. **16**, 6576 (2016).
[26] A. Brumberg, S. M. Harvey, J. P. Philbin, B. T. Diroll, S. A. Crooker, M. R. Wasielewski, E. Rabani, and R. D. Schaller, ACS Nano **13**, 8589 (2019).

[27]Q. Li, Y. Yang, W. Que, and T. Lian, Nano Lett. **19**, 5620 (2019).
[28]J. P. Philbin and E. Rabani, arXiv:1808.10404 (2020).
[29]L.-W. Wang, M. Califano, A. Zunger, and A. Franceschetti, Phys. Rev. Lett. **91**, 056404 (2003).
[30]M. Rohlfing and S. G. Louie, Phys. Rev. B **62**, 4927 (2000).
[31]S. Refaely-Abramson, F. H. Da Jornada, S. G. Louie, and J. B. Neaton, Phys. Rev. Lett. **119**, 267401 (2017).
[32]D. Neuhauser, E. Rabani, Y. Cytter, and R. Baer, J. Phys. Chem. A **120**, 3071 (2016).
[33]B. T. Diroll, I. Fedin, P. Darancet, D. V. Talapin, and R. D. Schaller, J. Am. Chem. Soc. **138**, 11109 (2016).
[34]A. Hazarika, I. Fedin, L. Hong, J. Guo, V. Srivastava, W. Cho, I. Coropceanu, J. Portner, B. T. Diroll, J. P. Philbin, E. Rabani, R. Klie, and D. V. Talapin, J. Am. Chem. Soc. **141**, 13487 (2019).
[35]F. Wang, Y. Wu, M. S. Hybertsen, and T. F. Heinz, Phys. Rev. B **73**, 245424 (2006).
[36]G. H. Bertrand, A. Polovitsyn, S. Christodoulou, A. H. Khan, and I. Moreels, Chem. Commun. **52**, 11975 (2016).
[37]D. E. Yoon, W. D. Kim, D. Kim, D. Lee, S. Koh, W. K. Bae, and D. C. Lee, J. Phys. Chem. C **121**, 24837 (2017).
[38]H. Zhao, S. Moehl, and H. Kalt, Phys. Rev. Lett. **89**, 097401 (2002).
[39]Q. Li and T. Lian, Acc. Chem. Res. **52**, 2684 (2019).
[40]X. Ma, B. T. Diroll, W. Cho, I. Fedin, R. D. Schaller, D. V. Talapin, S. K. Gray, G. P. Wiederrecht, and D. J. Gosztola, ACS Nano **11**, 9119 (2017).
[41]E. I. Rashba, Sov Phys Semicond **8**, 807 (1975).
[42]J. Feldmann, G. Peter, E. O. Göbel, P. Dawson, K. Moore, C. Foxon, and R. J. Elliott, Phys. Rev. Lett. **59**, 2337 (1987).
[43]A. W. Achtstein, A. Schliwa, A. Prudnikau, M. Hardzei, M. V. Artemyev, C. Thomsen, and U. Woggon, Nano Lett. **12**, 3151 (2012).
[44]M. Korkusinski, O. Voznyy, and P. Hawrylak, Phys. Rev. B **82**, 245304 (2010).
[45]D. Birkedal, J. Singh, V. G. Lyssenko, J. Erland, and J. M. Hvam, Phys. Rev. Lett. **76**, 672 (1996).
[46]J. Singh, D. Birkedal, V. Lyssenko, and J. Hvam, Phys. Rev. B **53**, 15909 (1996).
[47]D. B. Tran Thoai, R. Zimmermann, M. Grundmann, and D. Bimberg, Phys. Rev. B **42**, 5906 (1990).
[48]R. Benchamekh, N. A. Gippius, J. Even, M. O. Nestoklon, J. M. Jancu, S. Ithurria, B. Dubertret, A. L. Efros, and P. Voisin, Phys. Rev. B **89**, 035307 (2014).
[49]F. Rajadell, J. I. Climente, and J. Planelles, Phys. Rev. B **96**, 035307 (2017).

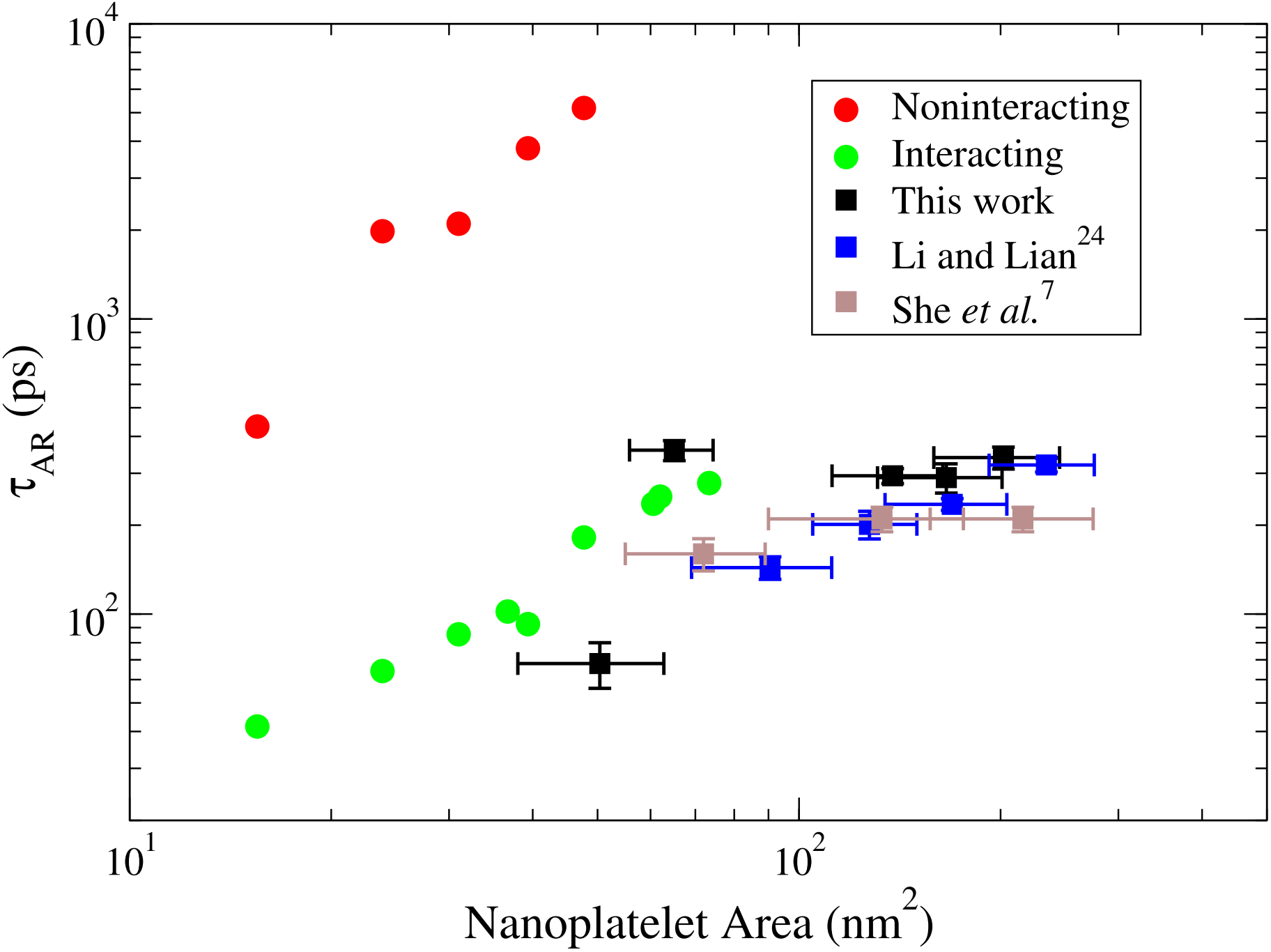
Noninteracting
Interacting
This work
Li and Lian[24]
She et al.[7]
τ_{AR} (ps)
Nanoplatelet Area (nm^2)
10^4
10^3
10^2
10^1
10^2

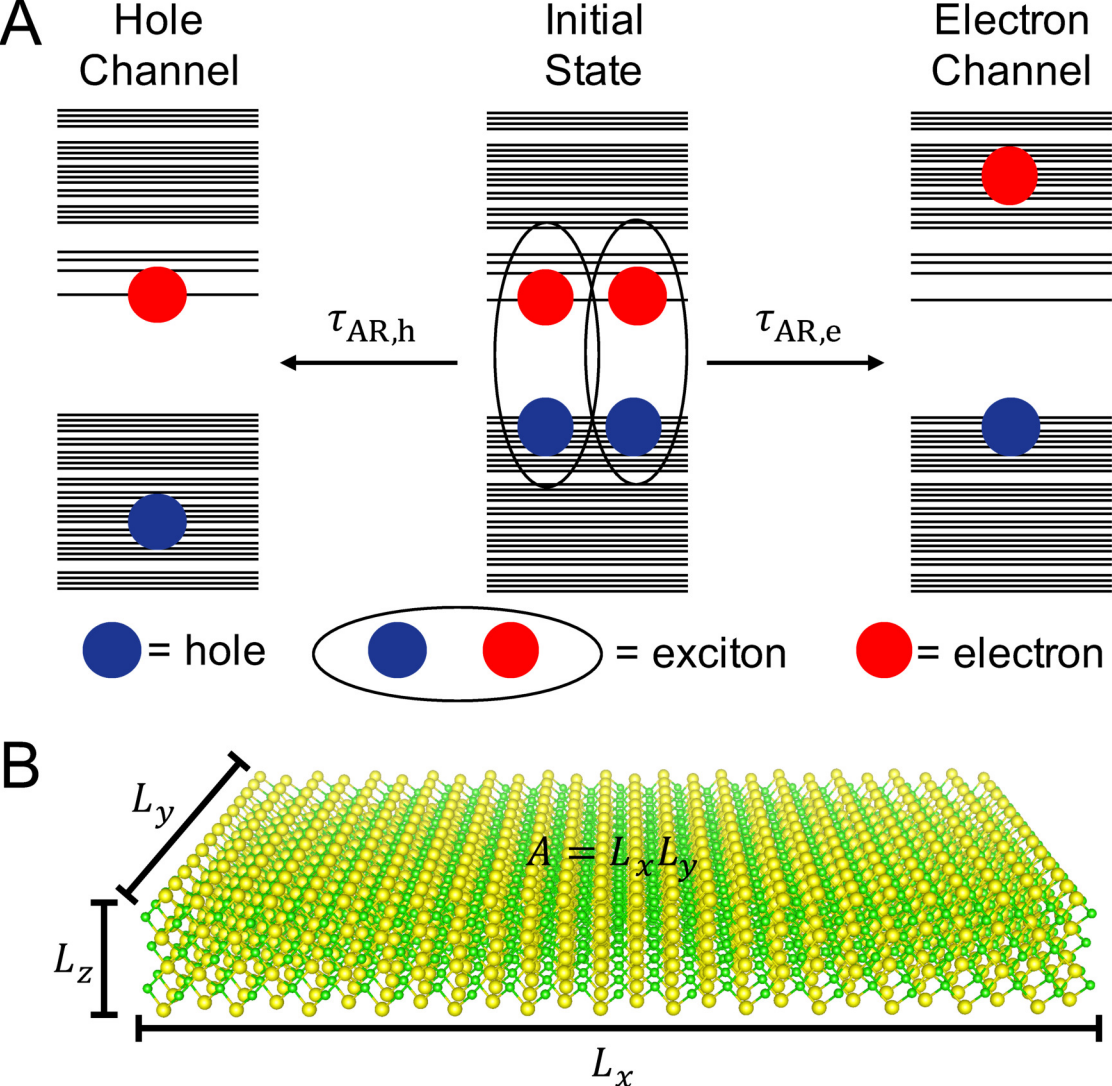
A
Hole Channel
Initial State
Electron Channel
$\tau_{AR,h}$
$\tau_{AR,e}$
= hole
= exciton
= electron
B
L_y
$A = L_x L_y$
L_z
L_x

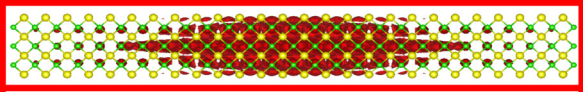
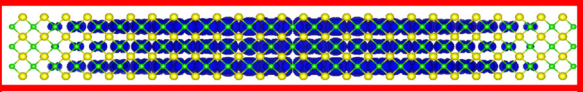
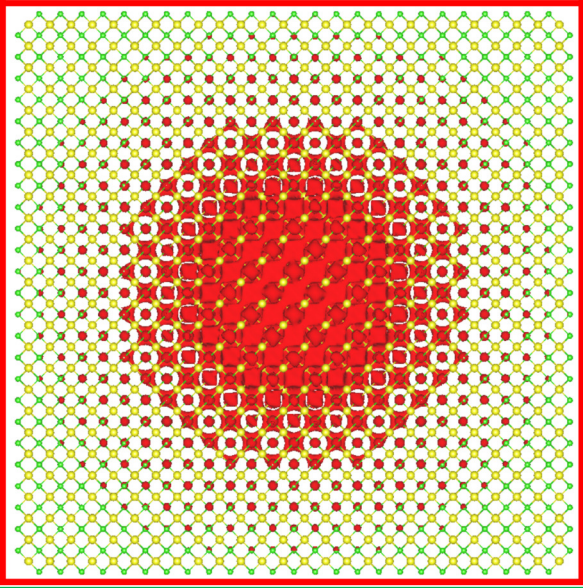
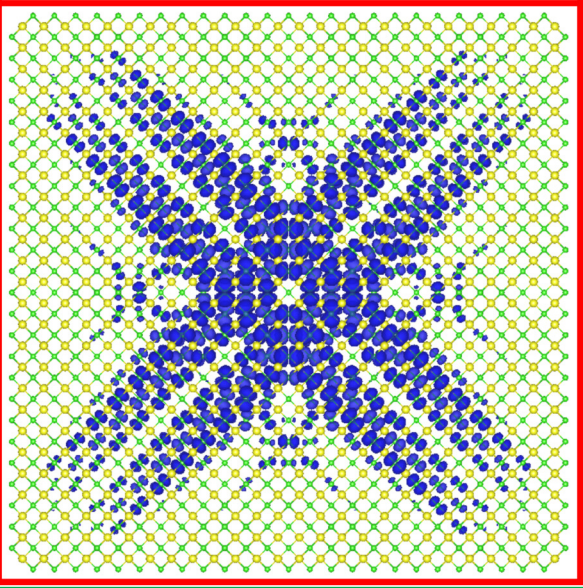
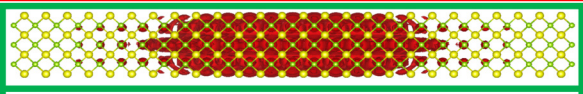
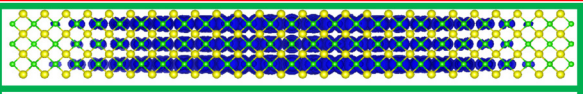
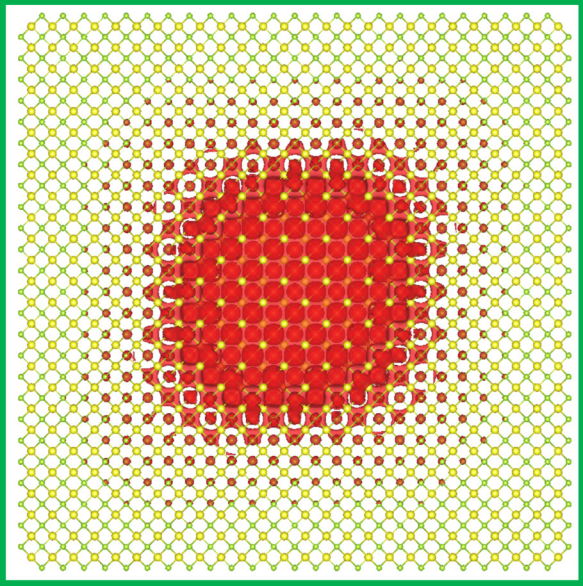
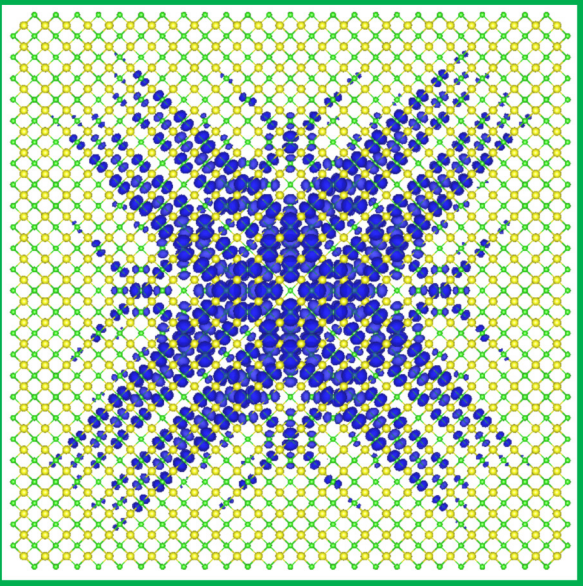

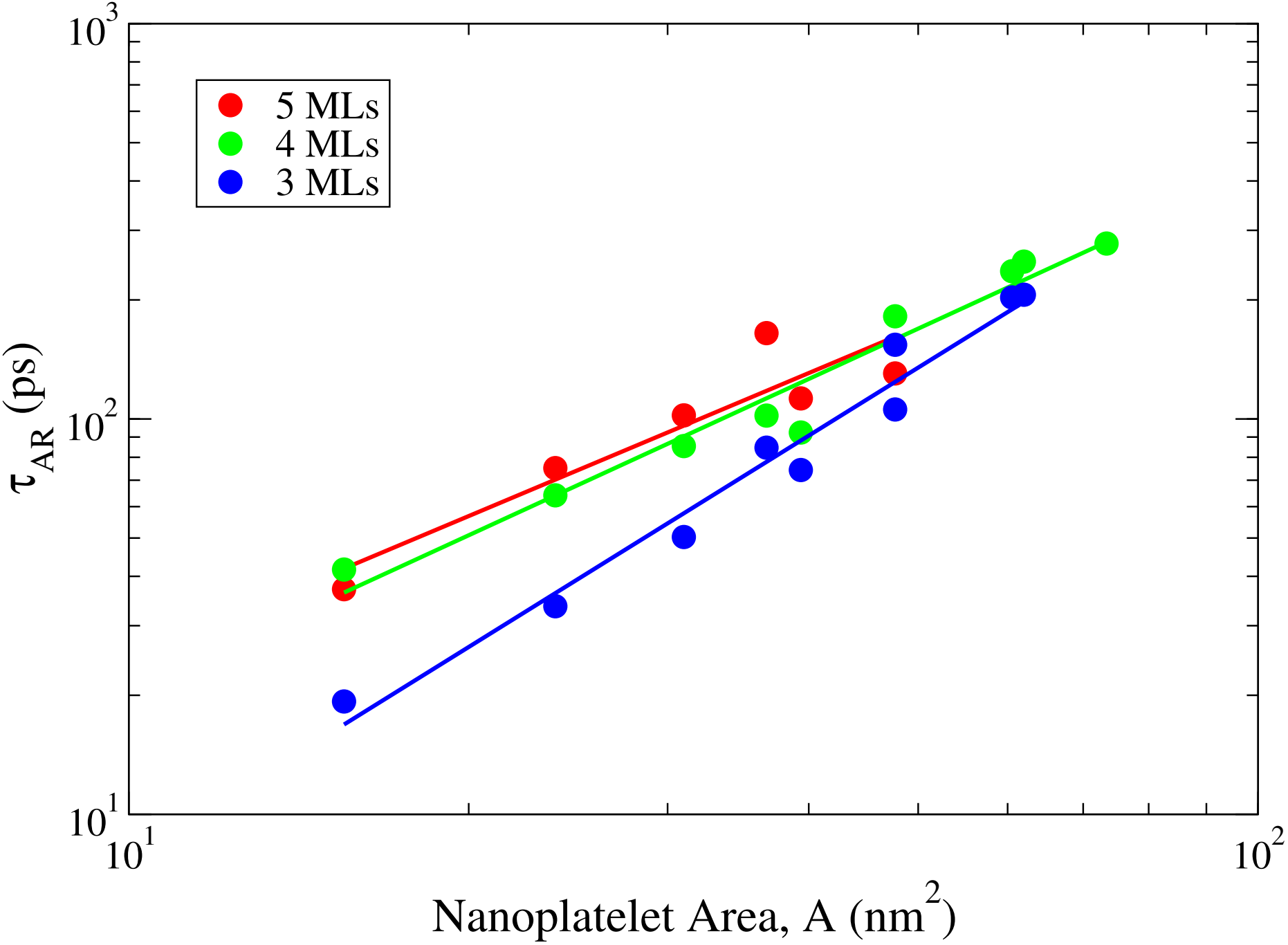
5 MLs
4 MLs
3 MLs
10^3
10^2
10^1
10^1
10^2
τ_{AR} (ps)
Nanoplatelet Area, A (nm^2)

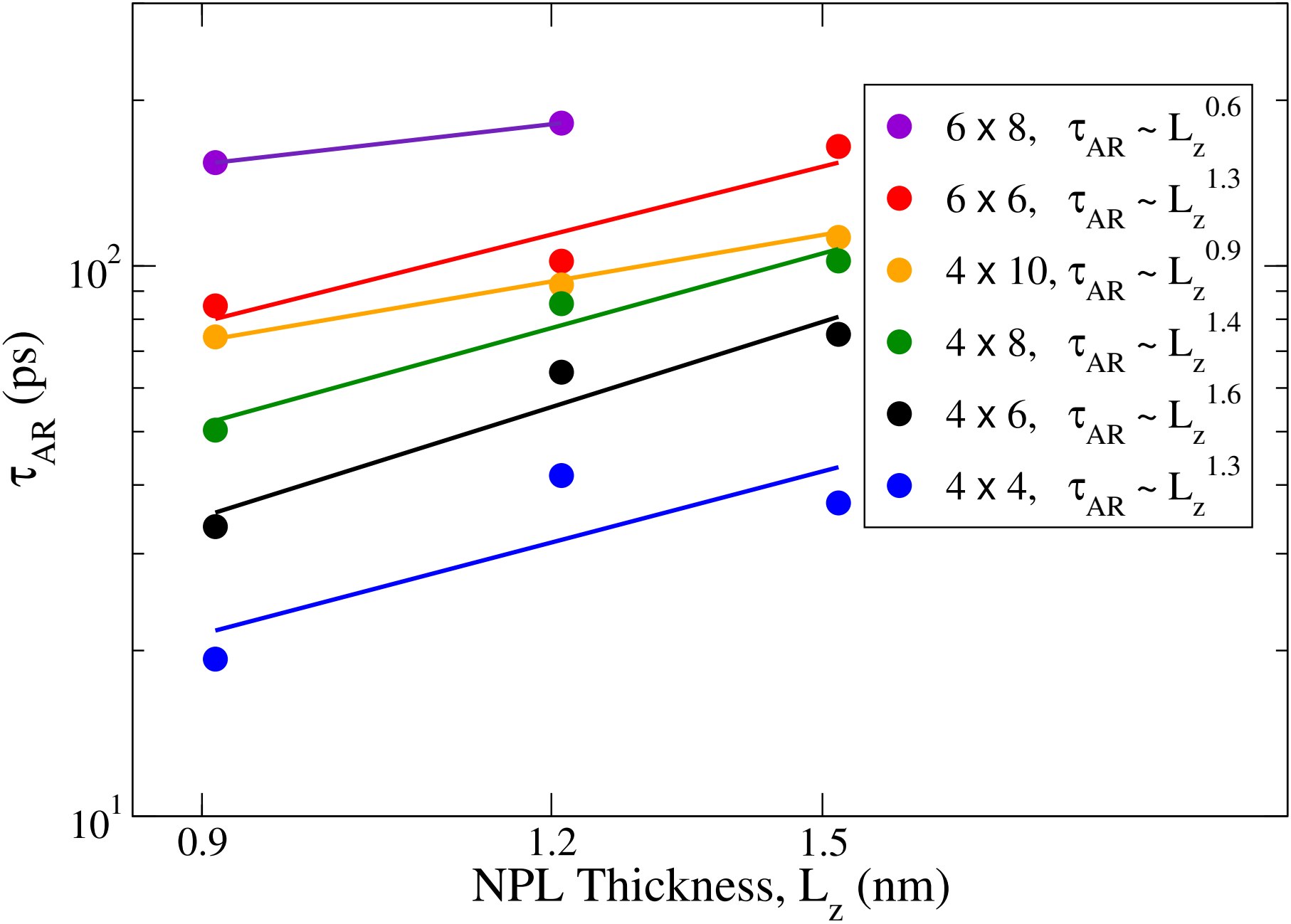
10^2
10^1
τ_{AR} (ps)
0.9
1.2
1.5
NPL Thickness, L_z (nm)
6 x 8, $\tau_{AR} \sim L_z^{0.6}$
6 x 6, $\tau_{AR} \sim L_z^{1.3}$
4 x 10, $\tau_{AR} \sim L_z^{0.9}$
4 x 8, $\tau_{AR} \sim L_z^{1.4}$
4 x 6, $\tau_{AR} \sim L_z^{1.6}$
4 x 4, $\tau_{AR} \sim L_z^{1.3}$

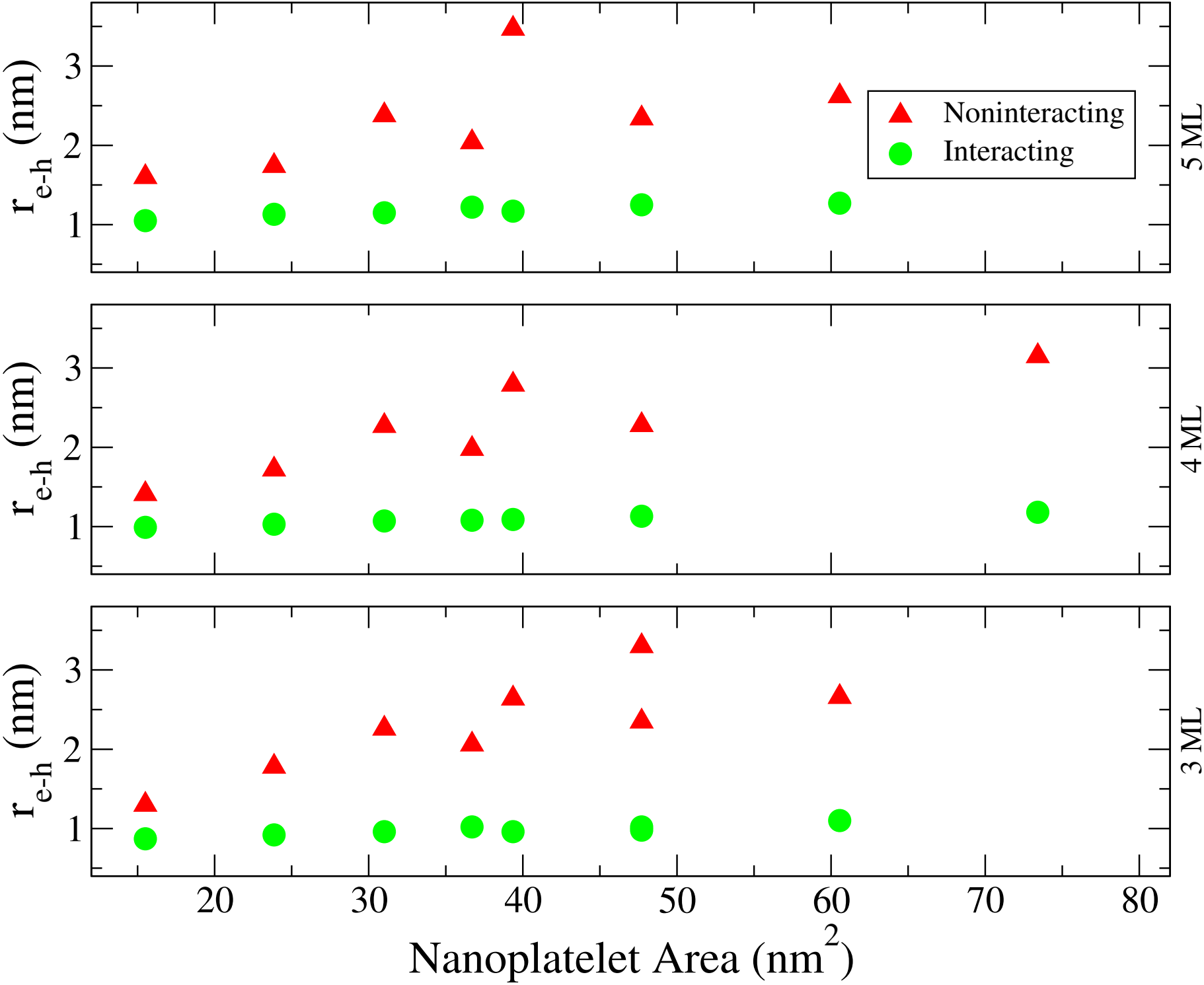
r e-h (nm)
1
2
3
Noninteracting
Interacting
5 ML
4 ML
3 ML
20
30
40
50
60
70
80
Nanoplatelet Area (nm2)